Cyclic Resistance, Pre and Post-Liquefaction Behavior of Dry Pluviated Silty Sands

Ali Shafiee

Geotechnical Engineering Research Center, International Institute of Earthquake Engineering and Seismology (IIEES), I.R. Iran, e-mail: shafieea@iiees.ac.ir

ABSTRACT: *The cyclic resistance along with pre and post-liquefaction behavior of mixtures of a saturated sand with varying amounts of a nonplastic silt are evaluated by cyclic triaxial tests, performed on undisturbed samples retrieved from calibration chamber and reconstituted samples prepared in laboratory utilizing dry pluviation method. Test results exhibit a clear trend between cyclic resistance and fines content in undisturbed specimens. The same trend is found in reconstituted specimens but with more scattering. Regardless of fines content, dilative behavior is observed in both types of specimens prior to liquefaction. Monotonic tests on reconstituted specimens also reveal the existence of dilative behavior. Indeed, increasing fines content would increase the post-liquefaction volumetric strain. The results of laboratory tests are also compared with cone penetration test (CPT) results. It is shown that strength reduction in CPT is much more than triaxial tests, when silt content is raised. Hence, fines tend to increase cyclic resistance ratio for the same normalized cone penetration resistance.*

Keywords: Silty sands; Cyclic resistance; CPT; Dilative; Volume change

1. Introduction

The effect of nonplastic fines on the liquefaction resistance of sands has been studied extensively in geotechnical literature. Mostly empirical correlations from in situ tests show that the presence of fines increases liquefaction resistance, e.g. [1-3], while the majority of laboratory tests show the opposite trend. Most of laboratory studies have reported that increasing silt content of a sand will either decrease the sand's resistance to liquefaction [4-10], or even the sand's resistance to liquefaction will initially decrease as the silt content increases until some minimum resistance is reached, and then increase as the silt content continues to increase [11-12]. In order to have a sound understanding of the liquefaction behavior of sand-silt mixtures, it is prudent to explore all features of the behavior thoroughly. This paper describes the results of an experimental study on the effect of nonplastic fines on the cyclic resistance, pre-liquefaction (i.e. dilative/ contractive) behavior and post-liquefaction (i.e. pore pressure dissipation and volume change) behavior of sands. To improve our understanding of liquefaction behavior of the mixtures, the results of cyclic triaxial tests are also compared with that of cone penetration test (*CPT*). All the tests were performed in different confining stresses to evaluate the effect of this parameter on the behavior as well.

Cyclic triaxial tests were run on both undisturbed samples retrieved from calibration chamber and reconstituted samples prepared in laboratory utilizing dry pluviation method. Triaxial tests were performed in different confining stresses on pure sand and silt specimens with silt additions of 10, 20, 30, 40 and 50% by weight. Following cyclic loading, pore pressure dissipation and volume change of undisturbed samples were also recorded to observe post-liquefaction behavior of silty sands. Furthermore, curves of cyclic resistance ratio (*CRR*) versus normalized cone penetration resistance, are developed from a combination of triaxial test results and *CPT* results previously performed by Ziaie-Moayed [13] on the same materials.

The novelty of this research program is that it investigates the following topics which have not been addressed clearly in the literature:

(a) Whether there exists any trend in the behavior of sand-silt mixtures (in terms of cyclic resistance) if no parameter (e.g., void ratio or sand skeleton void ratio) hold constant;
(b) The effect of initial confining stress on liquefaction behavior of sand-silt mixtures;
(c) The capability of calibration chamber alone for retrieving undisturbed samples and achieving *CPT* tests, and finally constructing -*CRR* relationship specially for sands containing high silt content;
(d) Post liquefaction behavior of sand-silt mixtures, specially at high silt content;
(e) Ability of cyclic triaxial tests to distinguish dilative behavior, and
(f) The effect of initial fabric on liquefaction behavior of sand-silt mixtures.

2. Experimental Program

The study described herein investigates the effects of nonplastic silt content on the cyclic resistance, pre and post-liquefaction behavior of a sand using isotropically-consolidated, undrained triaxial tests. Triaxial tests were performed on undisturbed samples retrieved from calibration chamber and also on reconstituted samples prepared in laboratory utilizing dry pluviation method. The systems used for conducting cyclic tests were advanced automated triaxial testing apparatus. In the triaxial cell, vertical load, pore pressure and axial deformation were measured with sensors of 500*kgf*, 10*kgf/cm*^{2} and 20*mm* capacity and an accuracy of 0.02*kg*, 0.004*kgf/cm*^{2} and 0.01*mm* respectively. A detailed description of the soils used, sample preparation technique and test procedure is given below.

2.1. Materials Tested

The sand used in the testing program was retrieved from a riverbed in the north of Tehran and composed of subangular aggregates. It is a medium quartizic sand and has a mean grain size, D50 of 0.43*mm*, coefficient of uniformity, *Cu* of 1.43 and a specific gravity of 2.66. The minimum and maximum void ratios of the sand are 0.614 and 1.015 respectively. The silt used in the study was derived by grinding the parent sand. The sand and silt are nonplastic, with no discernible liquid or plastic limit. Grain size distributions for the materials are presented in Figure (1).

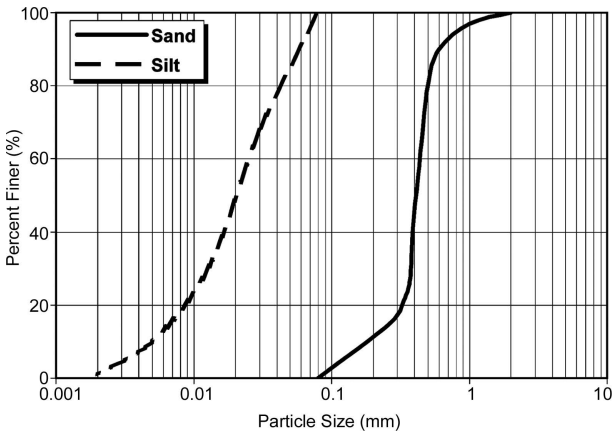

Figure 1. Grain size distributions for soils used in study.

Six combinations of sand and silt were created using the sand with silt additions of 0, 10, 20, 30, 40 and 50% by weight.

2.2. Specimen Preparation

One of the objectives of the present research was to study specimens prepared with a method that reproduced the natural deposits of silty sands. Since most sands that liquefy under different loading paths have been deposited under alluvial or marine conditions, a depositional method that simulates these low input energy depositional processes should be utilized. Dry pluviation has been shown to create a grain structure similar to that of naturally deposited river sands [14-15]. However, many of the water sedimentation depositional methods tend to produce inhomogeneous specimens. Therefore, the dry pluviation method was chosen as a reasonable depositional technique for the experimental program.

Two types of the samples were used to study liquefaction behavior of silty sands: undisturbed samples retrieved from calibration chamber and reconstituted samples prepared in laboratory utilizing dry pluviation method. To prepare undisturbed samples, the calibration chamber with a diameter of 75*cm* and a height of 150*cm* was firstly filled by the materials using dry pluviation method. More details of the sample preparation technique in calibration chamber can be found in [16]. Herein, a summary of the procedure followed is presented.

The materials in the calibration chamber were saturated and consolidated under different initial effective confining stresses of 100, 200 and 300*kPa*. The consolidated samples were then Frozen by a mechanical system. In general, it takes 3 to 4 days to freeze each sample. To prepare a specimen for triaxial

tests with a nominal diameter and height of 50 and 100 *mm* respectively, a cylinder with specified dimension was drilled in the materials. Then around the specimen was emptied carefully and the specimen was cut and prepared for triaxial testing. Care should be taken to minimize void ratio changes during the process of thawing. Herein, the method proposed by Vaid and Sivathayalan [17] was used. The method essentially consisted of allowing thawing to proceed with access to free water at both ends of the specimen, which allows for compensation of the volume deficiency caused by melting of pore ice. Thawing was done under a small effective stress of 20*kPa*.

To compare behavior of the undisturbed samples with the specimens prepared in the laboratory, second series of specimens were prepared in the laboratory by dry pluviation method. The specimens tested were typically 50*mm* in diameter and 100*mm* in height. The specimens were created by placing the dry materials into a funnel with a tube attached to the spout. The tube was placed at the bottom of a split-mould. The tube was slowly raised along the axis of symmetry of the specimen, such that the soil was not allowed any drop height. The sample preparation technique was found reliable when repeated testing of duplicate samples gave uniform results.

2.3. Test Procedure

Once the specimen had been formed, it was then saturated by flowing CO_2 and de-aired water through it, followed by the application of sufficient back pressure to ensure saturation. The specimens were then isotropically consolidated under three different initial effective confining stresses of 100, 200 and 300*kPa*. The values of void ratios presented herein are the values after consolidation. For practical purposes, target void ratios were not set identical for all type of the specimens.

The specimens were then loaded with a sinusoidal varying deviator stress at a constant cyclic stress ratio, *CSR* ($= \Delta s_1 / 2s'_C$, s_1 = axial stress, s'_C = initial effective confining stress) of 0.2 until they liquefied. The stress-controlled condition in the cyclic triaxial tests was applied with a frequency of 0.1*Hz* following the specifications of *ASTM* D5311 [18]. The loading rate for cyclic tests was also chosen so that pore pressure equalization through the specimen was ensured [19]. Cycles were set to start in compression loading for all tests. A deformation of 5% double amplitude axial strain was the criterion used in this study to define cyclic resistance of specimens of clean sands and sands containing fines [15].

Typical cyclic triaxial test results are presented in Figure (2). The data presented are from a test on an undisturbed specimen of sand with 50% silt content, at an initial effective confining stress of 100*kPa*. In the Figure deviatoric stress, excess pore pressure, and axial strain are each plotted against the number of cycles of loading. The specimen reached liquefaction at the end of the 11^{th} cycle.

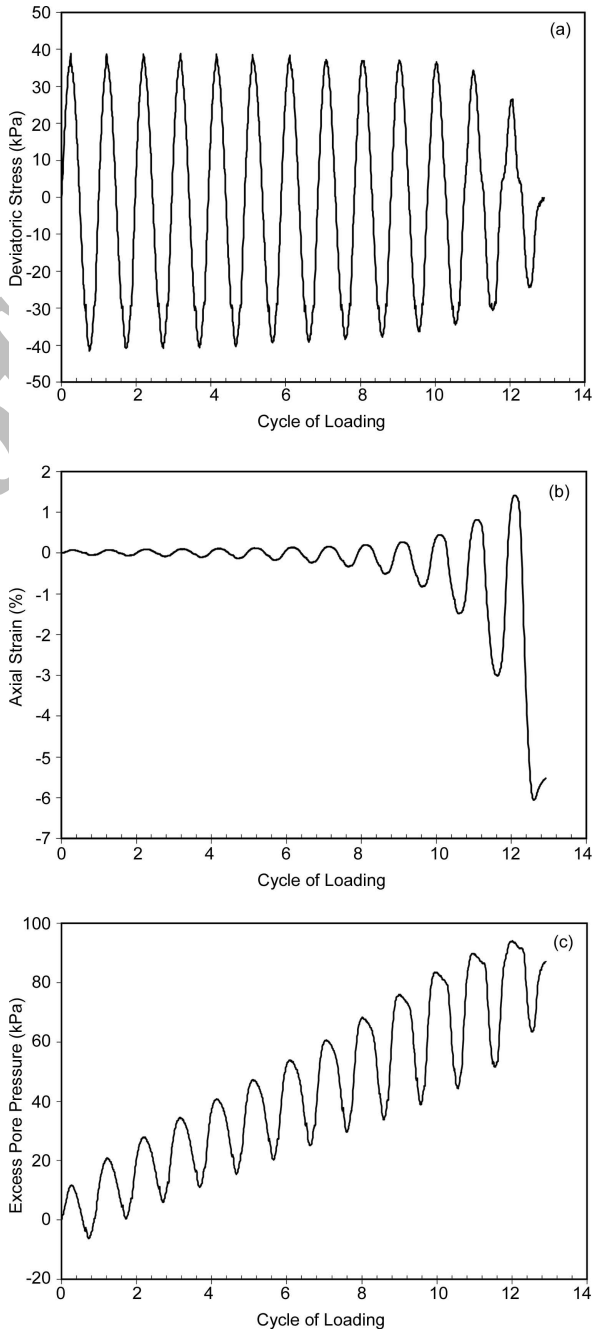

Figure 2. Typical cyclic triaxial test data, fines content=50%, σ'_C = 100kPa. (a) deviatoric stress vs number of cycles, (b) axial strain vs number of cycles, (c) excess pore pressure vs number of cycles.

To observe post-liquefaction behavior of the mixtures, once the specimen liquefied, the cyclic loading phase was terminated and volume change and pore pressure dissipation were measured immediately. The bottom end of the specimen was connected to a volume measuring burette. The top end of the specimen was connected to a pore pressure transducer with no drainage allowed from this end. This setup simulated a one-way drainage condition. The dissipation measurements were only carried out for the undisturbed specimens.

3. Evaluation of Cyclic Resistance

The cyclic resistance determined for the various combinations of sand and silt are examined in terms of their silt content. Figure (3) presents cyclic resistance expressed in terms of number of cycles to liquefaction, N_l versus silt content in undisturbed and reconstituted specimens for different initial confining stresses. As may be seen in Figure (3), (although there is somewhat more scatter in the data of reconstituted specimens) regardless of the confining stress, the cyclic resistance generally decreases as the silt content increases until a minimum cyclic resistance is reached at a limiting silt content. As the silt content continues to increase above this limit, the cyclic resistance increases. The limiting silt content seems to be 40% for undisturbed specimens and somewhat less than 40% for reconstituted specimens. The observed trend is consistent with the previous studies which show a decrease in cyclic resistance with increasing silt content, until reaching the limiting silt content after which cyclic resistance increases, e.g. [11-12].

A comparison on the cyclic resistance of the specimens reveals, that although reconstituted specimens have less void ratio in comparison to undisturbed specimens, see Tables (1) and (2), their cyclic resistance is generally less than undisturbed specimens, see Figure (3). Referring to Table (1), for example, in undisturbed specimens of sands containing 20% fines, void ratio ranges from 0.832 to 0.717, and N_l varies from 13 to 17. Meanwhile in reconstituted specimens of the same mixture, with lower void ratios (from 0.802 to 0.705), N_l ranges from 5 to 11, see Table (2). It may be inferred that relying on the results of laboratory tests on dry deposited reconstituted specimens is conservative. Figure (3) also shows that when fines content is raised the difference between cyclic resistance of undisturbed and reconstituted specimens is decreased. The difference may be due to some cementation or weak cohesion occurring during the consolidation.

Regarding the effect of initial confining stress on cyclic resistance, Figure (3a) shows that for both undisturbed and reconstituted specimens at low confining stress (i.e. 100*kPa*), specimens containing 10% silt content exhibit a little higher cyclic resistance than clean sands, while this trend diminishes gradually when confining stress is raised (e.g., at 300*kPa*).

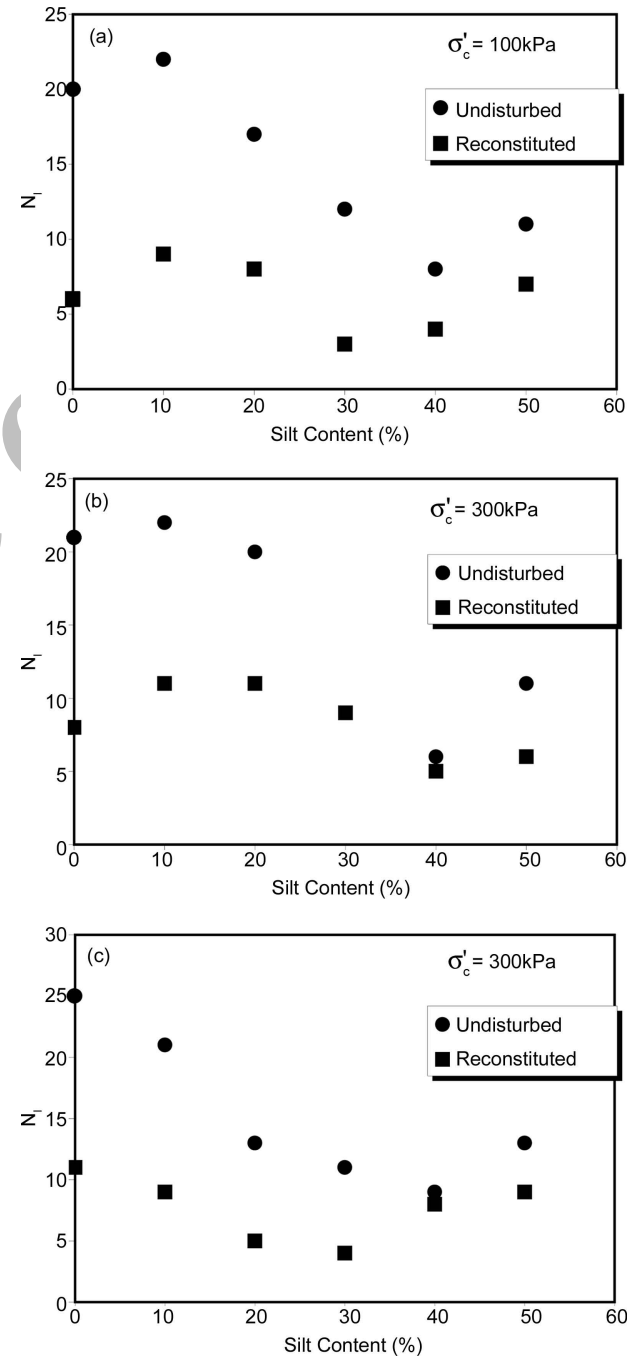

Figure 3. Variation in N_l with silt content for undisturbed and reconstituted specimens.

Table 1. Test conditions and results for the cyclic triaxial tests conducted on undisturbed specimens.

Fines Content (%)	Initial Confining Stress (kPa)	Void Ratio	Sand Skeleton Void Ratio	No. of Cycles to Liquefaction (N_l)
0	100	0.934	0.934	20
	200	0.910	0.910	21
	300	0.865	0.865	25
10	100	0.876	1.084	22
	200	0.867	1.026	22
	300	0.791	0.990	21
20	100	0.832	1.290	17
	200	0.811	1.213	20
	300	0.717	1.146	13
30	100	0.783	1.547	12
	200	0.720	1.457	9
	300	0.694	1.420	11
40	100	0.752	1.920	8
	200	0.693	1.821	6
	300	0.665	1.775	9
50	100	0.707	2.414	11
	200	0.686	2.372	11
	300	0.652	2.304	13

Table 2. Test conditions and results for the cyclic triaxial tests conducted on reconstituted specimens.

Fines Content (%)	Initial Confining Stress (kPa)	Void Ratio	Sand Skeleton Void Ratio	No. of Cycles to Liquefaction (N_l)
0	100	0.864	0.864	6
	200	0.815	0.815	8
	300	0.782	0.782	11
10	100	0.823	1.026	9
	200	0.804	1.004	11
	300	0.796	0.996	9
20	100	0.802	1.253	8
	200	0.736	1.170	11
	300	0.705	1.131	5
30	100	0.728	1.469	3
	200	0.692	1.417	9
	300	0.678	1.397	4
40	100	0.710	1.850	4
	200	0.683	1.805	5
	300	0.651	1.752	8
50	100	0.700	2.400	7
	200	0.652	2.304	6
	300	0.631	2.262	9

4. CPT-Based Liquefaction Resistance

The effect of fines content on the liquefaction resistance of sand-silt mixtures has received increased attention during the past 20 years and a considerable amount of data is available in the technical literature. However, much of these data, specially comparing in situ studies with laboratory ones, are contradictive and subject seems to be associated with confusion. For instance, in the simple geotechnical criterion depicted in the diagram of Figure (4) (proposed by Stark and Olson [2]), cyclic resistance ratio for 7.5-magnitude earthquake, $(CRR)_{7.5}$ required to initiate liquefaction for a given value of q_{c1}, increases with increasing fines content, and *FC* indicating that the fines tend to inhibit liquefaction. Meanwhile as mentioned previously, most of the laboratory studies including test results presented herein, show the reverse trend, see Figure (3).

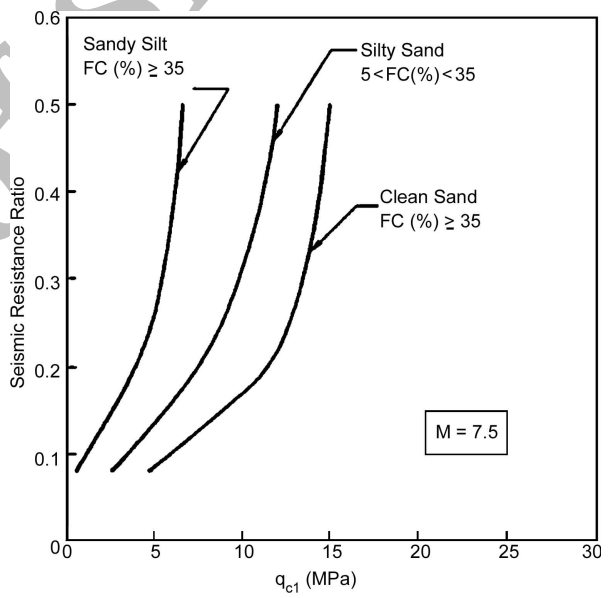

Figure 4. CPT-Based liquefaction-potential relationships for sand-silt mixtures and M=7.5 earthquakes [2].

In order to have a better understanding of the liquefaction behavior of silty sands tested in this study, laboratory test results on undisturbed specimens are compared with the *CPT* results, previously performed in the calibration chamber by Ziaie-Moayed [13] on the same mixtures and at the same confining stresses. It should be noted that the difference between the after consolidation void ratio of undisturbed specimens and that of the soils tested in the calibration chamber, is less than 10% [19].

A water tank installed at 2.5*m* above ground surface was used to provide required water-head for saturation of the material in the calibration chamber.

The required pressure for consolidation of the material was also supplied by a compressor. Piezocone used for *CPT* has a capacity of 100*kN*. It provides the continuous measurement of cone penetration resistance, frictional resistance, pore water pressure and its inclination with respect to vertical. In order to perform the test, the piezocone, was installed on a frame, with its direction along the centerline of the chamber. Having finished the saturation and consolidation process, the *CPT* was performed with a velocity of 2*cm/s* [20].

Table (3) presents the values of q_{c1} for the mixtures. The values of q_{c1} are obtained by normalizing cone penetration resistance, q_c through the following equation [21]:

$$q_{c1} = \frac{1.8}{0.8 + \sigma'_{v0} / \sigma_{ref}} q_c \quad (1)$$

where σ'_{v0} is initial effective vertical pressure in terms of kPa and reference stress, σ_{ref} is equal to 96*kPa*. Figure (5) shows variation of q_{c1} in terms of silt content. As can be seen, regardless of confining stress, q_{c1} decreases when silt content is raised. The trend shown in Figure (5) is generally consistent with the trends obtained in laboratory tests, see Figure (3). This means that increasing silt content will generally cause a looser fabric to be formed.

Table 3. Values of normalized cone penetration resistance, q_{c1} and cyclic resistance ratio for 7.5-magnitude earthquake, $(CRR)_{7.5}$.

Fines Content (%)	Initial Effective Confining Stress (kPa)	q_{c1} (MPa)	$(CRR)_{7.5}$
0	100	1.56	0.11
	200	2.18	0.12
	300	1.83	0.12
10	100	1.37	0.12
	200	1.87	0.12
	300	1.56	0.12
20	100	1.17	0.11
	200	1.37	0.11
	300	1.28	0.10
30	100	0.78	0.10
	200	0.91	0.09
	300	1.15	0.10
40	100	0.64	0.09
	200	0.75	0.08
	300	1.10	0.09
50	100	0.59	0.10
	200	0.69	0.10
	300	1.01	0.10

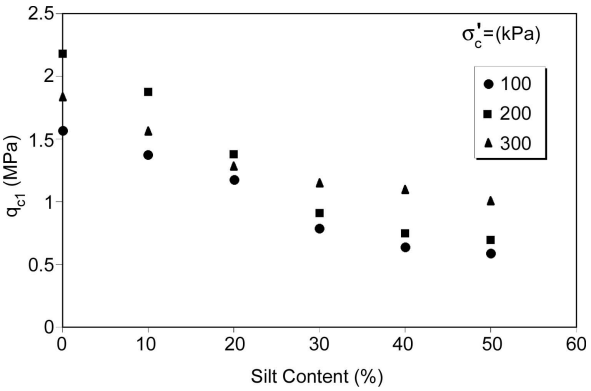

Figure 5. Variation in normalized cone penetration resistance, q_{c1} (MPa) with silt content.

To construct a relation between $(CRR)_{7.5}$ and q_{c1}, first the value of field cyclic resistance ratio, $(CRR)_{field}$ is computed as:

$$(CRR)_{field} = \alpha\beta(CSR) \quad (2)$$

in which α is a correction factor accounting for the different loading conditions in cyclic triaxial and cyclic simple shear apparatus, β is a correction factor incorporating effect of multidirectional shaking in the field and *CSR* is 0.2 for all of the mixtures, as previously mentioned. In this study, the value of α is taken as 0.6 [22] and the value of β is considered as 0.9 [23].

Having obtained the values $(CRR)_{field}$ and N_l, see Table (1), the value of $(CRR)_{7.5}$ is calculated as follows:

$$(CRR)_{7.5} = (CRR)_{field} / MSF \quad (3)$$

where *MSF* is magnification scaling factor, developed by Seed and Idriss [24], from average numbers of loading cycles to liquefaction for various earthquake magnitudes, *M* and laboratory test results, see Figure (6). Figure (6) represents a curve correlating the number of loading cycles required to generate liquefaction for a given cyclic stress ratio, *CSR* and for various magnitudes of earthquakes. Based on this figure, for example, for a specimen which is liquefied at 26^{th} cycle in the laboratory, *MSF* will be 0.89. As may be seen, herein $(CRR)_{7.5}$ is defined as the cyclic stress ratio required to cause liquefaction in 15 cycles of loading. Table (3), presents the values of $(CRR)_{7.5}$ for different mixtures, computed on the basis of the mentioned procedure.

Figure (7) shows variation of $(CRR)_{7.5}$ with respect to q_{c1} for different sand-silt mixtures. To facilitate comparison of $(CRR)_{7.5}$ for different

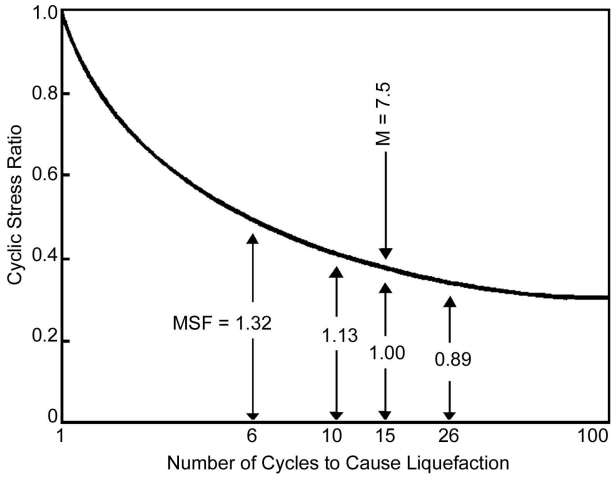

Figure 6. Representative relationship between CSR and number of cycles to cause liquefaction [24].

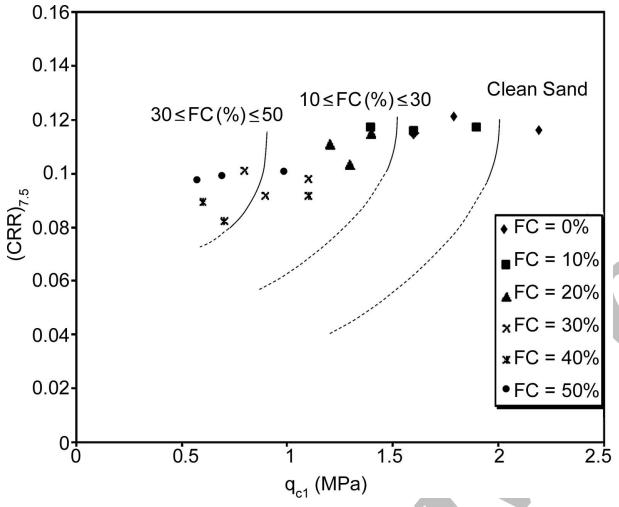

Figure 7. Proposed correlations between cyclic resistance ratio for 7.5-magnitude earthquake, $(CRR)_{7.5}$ and normalized cone penetration resistance, q_{c1} for sand-silt mixtures.

mixtures, lines were passed through each set of data. However, more data is needed to plot the trends accurately. The trends shown in Figure (7) are generally in accordance with the previous studies, indicating that, the fines tend to increase liquefaction resistance. It is interesting to note when fines content is raised, q_{c1} is reduced much more than $(CRR)_{7.5}$. Referring to Table (3), for example, $(CRR)_{7.5}$ of a specimen containing 40% fines, is 20% less than that of clean sand for an initial confining stress of 100*kPa*, but the q_{c1} of the same specimen at the same initial confining stress is 60% less than that of clean sand. Thus, for the same q_{c1}, when fines content is raised, $(CRR)_{7.5}$ increases, see Figure (7).

The procedure outlined in this study, i.e., the capability of calibration chamber alone for retrieving undisturbed samples and achieving *CPT* tests, and finally constructing q_{c1} - $(CRR)_{7.5}$ relationship, is a powerful tool for generating data especially where the data is rare. This, for instance, includes various soil mixtures, soil fabrics, confining stresses and boundary conditions.

5. Pre-Liquefaction Behavior of Silty Sands

To have more insight on the behavior of dry pluviated sand-silt mixtures, herein the contractive/ dilative behavior of sand-silt mixtures is investigated. Figure (8) shows the variation of pore pressure normalized by the initial confining stress in terms of cycles of loading for undisturbed specimens tested at a confining stress of 200*kPa* (although not shown herein, the behavior for other confining stresses is the same). As seen for all the mixtures, pore pressure increases as loading proceeds. However, the trend of pore pressure generation changes at a few cycles prior to liquefaction. This change in pore pressure variation which hereafter is called "splitting" and noted on Figure (8), is an indication of the dilative behavior. Figure (9) typically presents the stress-path for the specimen containing 30% fines in the $p'-q'$ plane, where $p'=\frac{\sigma'_1+2\sigma'_3}{3}$ and $q'=\sigma'_1-\sigma'_3$ (σ'_1 and σ'_3 are the principal effective stresses). In Figure (9), for example, the points on the stress-path of a specimen containing 30% fines (σ'_C =200*kPa*), after which the behavior changes from contractive to dilative, were marked and phase transformation line, *PTL* [15] was drawn. Although not shown herein, the dilative behavior is also seen for reconstituted specimens [19]. In order to locate more accurately the *PTL*, the values of p' and q' at the phase transformation state were obtained for the mixtures at each confining stress. Figure (10a) presents the values of PTL in the $p'-q'$ plane in undisturbed specimens. As seen, all data points fall within a narrow range and hence, *PTL* can be fitted to the data, passing through origin. The slope of *PTL* may be computed as 1.12. Figure (10b) also shows the values of p' and q' at the phase transformation state in reconstituted specimens. Herein, the slope of *PTL* can be computed as 1.18. This demonstrates that the slope of *PTL* is nearly independent of initial fabric. The difference in initial fabric can be attributed to the fact that the samples retrieved from calibration chamber are not truly undisturbed owing to the sampling method and reconsolidation of the material. However, the scanning microscopic electron may be needed to confirm the difference in initial fabric.

To confirm the existence of dilative behavior, monotonic tests were run on the reconstituted specimens at different initial confining stresses of 100, 200 and 300 kPa. Figure (11) shows the stress-path in the $p'-q'$ plane. Referring to Figure (11), dilative behavior is seen for all specimens. It can be shown that the dilative behavior, in general, begins at axial strains from 1.5 to 3.3% and continues to the end of

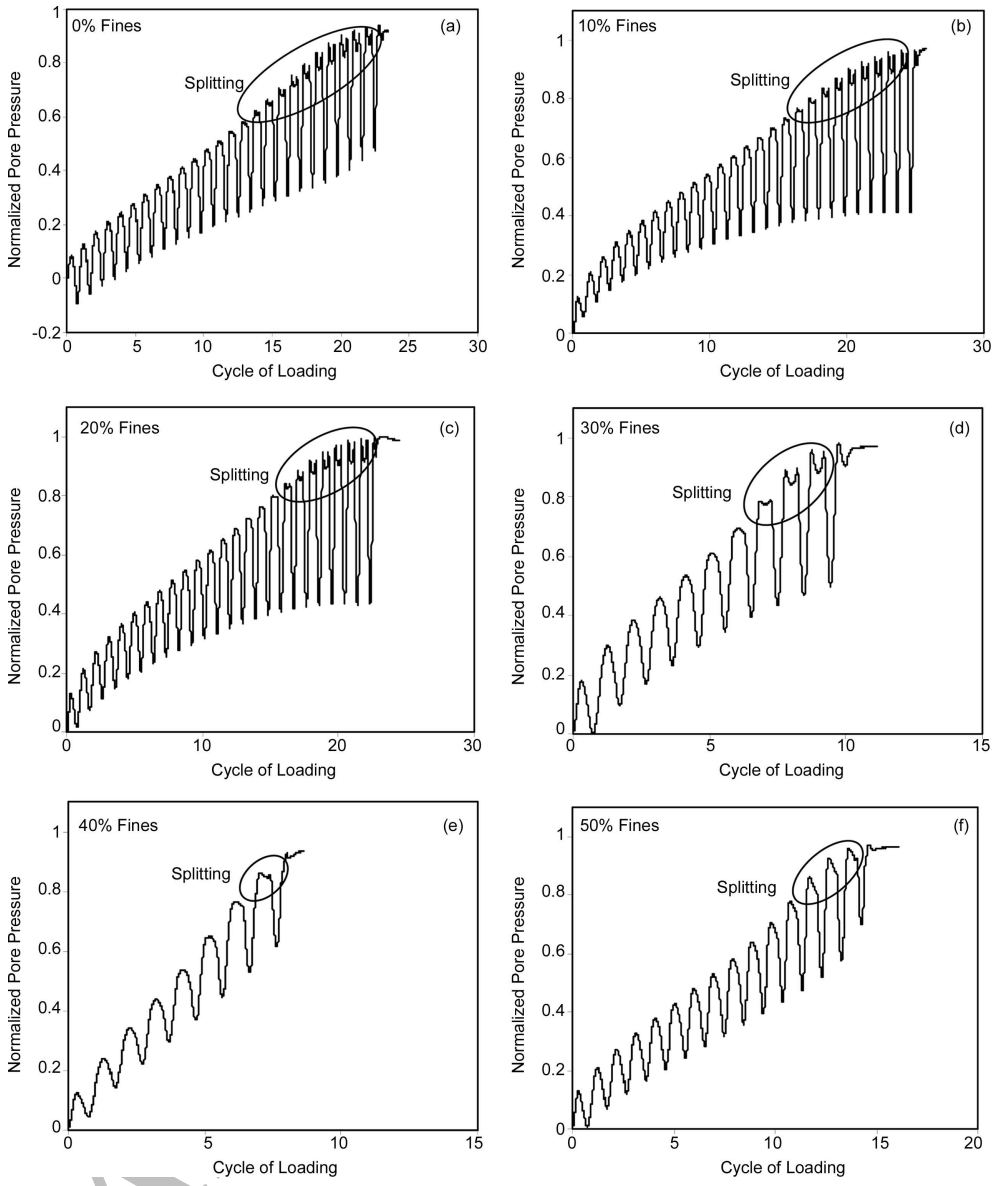

Figure 8. Variations of normalized pore pressure in undisturbed specimens of sand-silt mixtures, $\sigma'_C = 200$kPa.

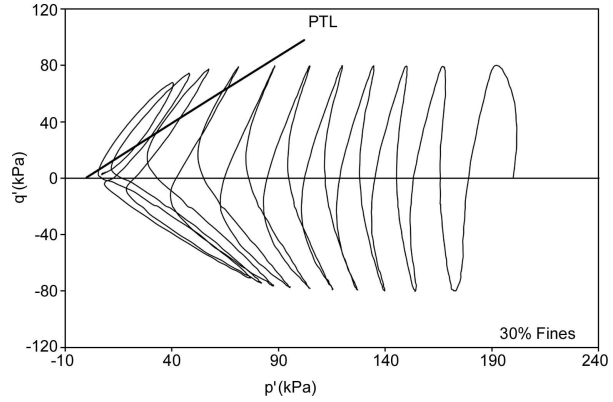

Figure 9. Stress-path in $p'-q'$ plane for the undisturbed specimen containing 30% fines, $\sigma'_C = 200$kPa.

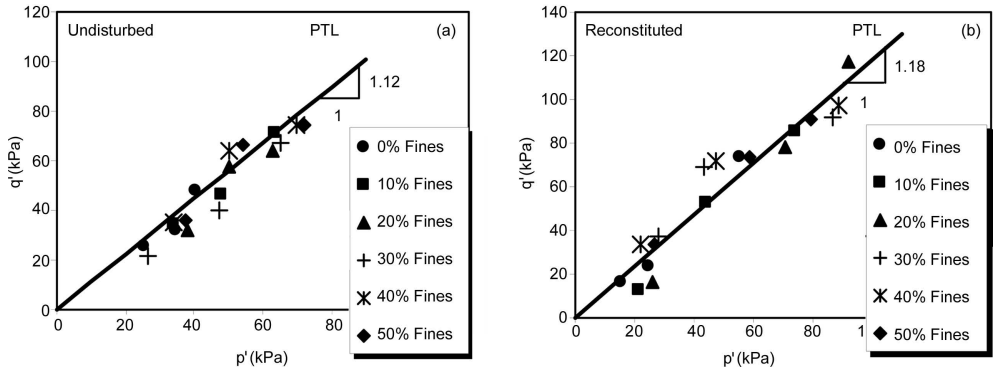

Figure 10. The values of p' and q' at phase transformation state.

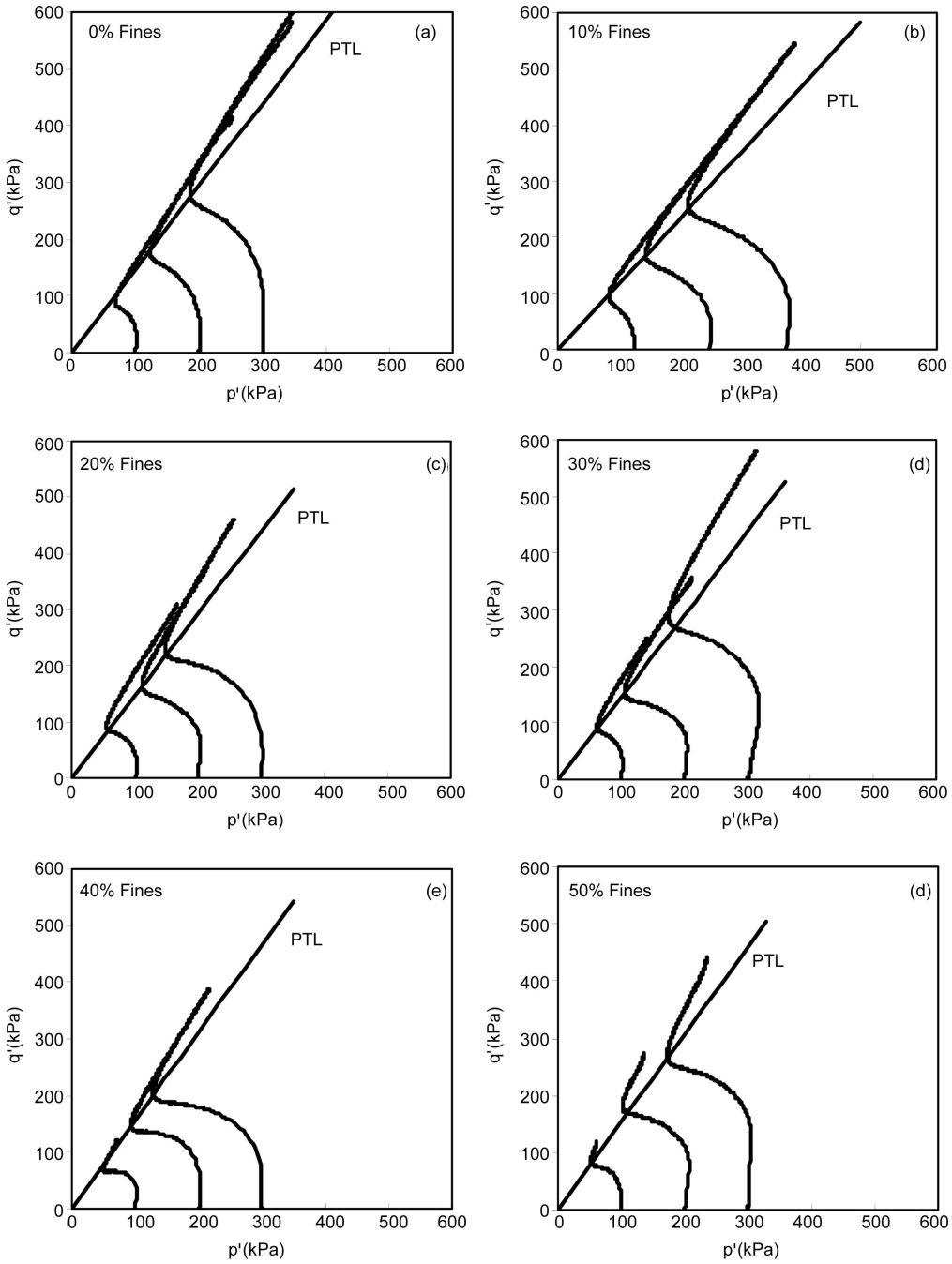

Figure 11. Stress-path in $p'-q'$ plane for monotonic tests performed on reconstituted specimens.

the tests [19]. Shown in Table (4), are the values of slope of *PTL* obtained from monotonic tests. As seen, the slope of *PTL* is nearly independent of fines content. However, the slope obtained from monotonic tests is more than that of cyclic tests.

Table 4. Slope of PTL obtained from monotonic tests run on reconstituted specimens.

Fines Content (%)	Slope of PTL
0	1.46
10	1.46
20	1.47
30	1.46
40	1.55
50	1.53

6. Post-Liquefaction Response of the Sand-Silt Mixtures

Detailed understanding of the post-liquefaction behavior of the sand-silt mixtures, including pore pressure dissipation and densification characteristics can give insight to the behavior of the silty sands. It can also be used for evaluation of post-liquefaction settlement and design of drainage systems to mitigate liquefaction. At present, there is only limited data available on this subject [25-30]. The data is primarily limited to clean sands, although recently Thevanayagam and Martin [31] studied the post-liquefaction behavior of silty soils.

To observe post-liquefaction behavior of the mixtures, once the specimen liquefied, the cyclic loading phase was terminated and volume change and pore pressure dissipation were measured immediately. Volume change was measured from the bottom end of the specimen, whilst pore pressure was measured from the top end of the specimen. The dissipation measurements were only carried out for the undisturbed specimens. Figure (12) shows the variation of dissipated post-liquefaction pore pressure versus time for $\sigma'_C = 200kPa$ (although not shown herein, the behavior for other confining stresses is the same). As may be seen, when silt content is raised, the required time for dissipation of the generated pore pressure is also increased. For example, specimens containing 50% fines require more time to dissipate all the generated pore pressure with respect to specimens containing 10% silt content. The observed trend is logical, since void ratio and subsequently permeability decrease when silt content is raised.

Figure (13) shows the post-liquefaction densification data for the same specimens. The figure

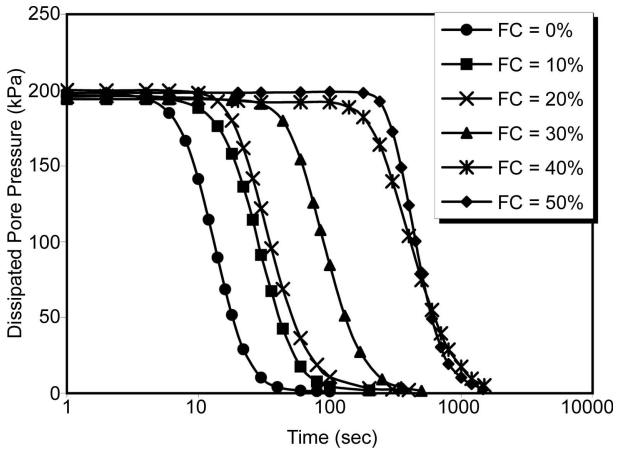

Figure 12. Variation of dissipated pore pressure vs time in undisturbed specimens of sand-silt mixtures, $\sigma'_C = 200kPa$.

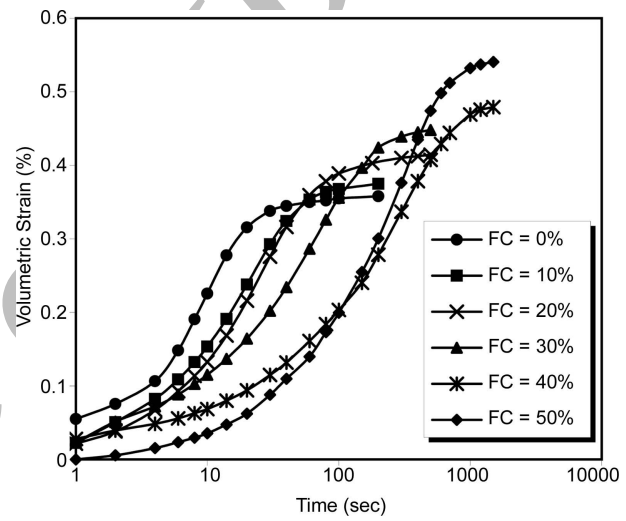

Figure 13. Variation of the volumetric strain vs time in undisturbed specimens of sand-silt mixtures, $\sigma'_C = 200kPa$.

presents variation of the volumetric strain (i.e. volume of water expelled out of the specimen divided by the end of consolidation volume of the specimen) versus time for different specimens. The Figure shows that in all specimens volumetric strain increases with time, until reaching a constant value (i.e. final volumetric strain). However, for specimens containing more fines, because of the lower permeability, the time needed to reach the final volumetric strain increases. An interesting feature of post-liquefaction behavior which can be found in Figure (13), is that higher final volumetric strain would be attained when silt content is raised. This means that increasing silt content causes a looser fabric to be formed. This finding is generally in accordance with the data previously shown on cyclic resistance, see Figure (3), and *CPT*, see Figure (5) of silty sands.

Figure (14) also shows that there exists a strong correlation between sand skeleton void ratio and final volumetric strain. Sand skeleton void ratio is one that exists in a silty sand if all of the silt particles were removed, leaving only the sand grains and voids to form the sand skeleton, see Table (1). As seen in Figure (14), final volumetric strain increases linearly with increasing sand skeleton void ratio. It may be inferred that sand skeleton void ratio can successfully describe the post-liquefaction behavior.

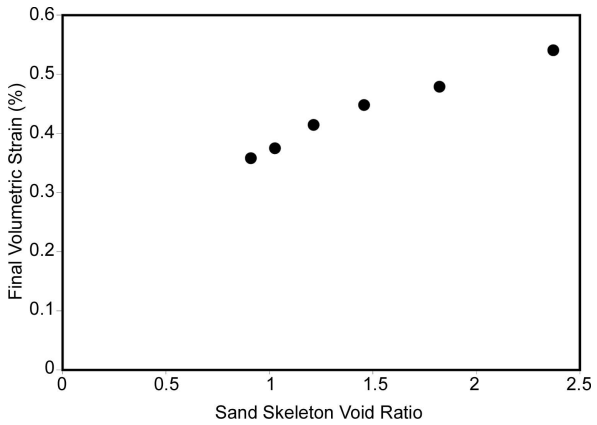

Figure 14. Variation in final volumetric strain with sand skeleton void ratio for undisturbed specimens, $\sigma'_C = 200$kPa.

7. Summary and Conclusions

The results of an experimental study on the liquefaction behavior of undisturbed and reconstituted specimens of nonplastic sand-silt mixtures at different initial effective confining stresses were presented. Cyclic resistance, pre and post-liquefaction behavior of the mixtures were investigated. The results of cone penetration tests (*CPT*) were also used to assist in better understanding of the behavior. The following conclusions regarding the effects of nonplastic fines on the liquefaction susceptibility of sands can be drawn from this study:

- In both undisturbed and reconstituted specimens, regardless of the initial confining stress, the cyclic resistance decreases as the silt content increases until a minimum cyclic resistance is reached at a limiting silt content. The limiting silt content is 40% for undisturbed specimens and somewhat less than 40% for reconstituted specimens. As the silt content continues to increase above limiting silt content, the cyclic resistance increases. In addition, undisturbed specimens exhibit higher cyclic resistance than reconstituted specimens, although their void ratio is higher than that of reconstituted specimens. When fines content is raised, the difference between cyclic resistance of undisturbed and reconstituted specimens is reduced.
- Initial effective confining stress can affect the cyclic resistance, especially at low fines content. At low confining stresses, specimens containing 10% silt content exhibit a little higher cyclic resistance than clean sands, while this trend diminishes gradually when confining stress is raised.
- Normalized cone penetration resistance, q_{c1} decreases when silt content is raised. Meanwhile correlation between cyclic resistance obtained from laboratory tests and q_{c1} shows that for the same q_{c1}, the fines tend to increase liquefaction resistance. It can be concluded that when silt content is raised, the strength reduction during *CPT* is much more than laboratory tests.
- In cyclic loading, undisturbed and reconstituted specimens show dilative behavior prior to liquefaction. Monotonic tests performed on reconstituted specimens also reveal the dilative behavior. Furthermore, the slope of phase transformation line is independent of both initial fabric and fines content. However, the slope obtained from monotonic tests is more than that of cyclic tests.
- When silt content is raised, the required time for dissipation of the post-liquefaction pore pressure is increased. Furthermore, increasing fines content leads to more final volumetric strain. In this regard, sand skeleton void ratio can describe the post-liquefaction behavior well.
- In general, when fines content is raised, the stability of the mixture fabric is reduced. Data obtained on cyclic resistance, *CPT* and post-liquefaction behavior of the mixtures evidently show that, in general, increasing fines content lead to less cyclic strength, less cone penetration resistance and higher post-liquefaction volumetric strain.

Acknowledgements

This study was supported by International Institute of Earthquake Engineering and Seismology (*IIEES*). Grateful appreciation is expressed for this support. The author also wishes to thank Dr. M. Asna-Ashari (who managed most of the tests), Dr. M.K. Jafari and Dr. M.H. Baziar for their excellent contributions in this study. The assistance of Mr. O. Norouzi with some of the tests is also appreciated.

References

1. Seed, H.B., Tokimatsu, K., Harder, L.F., and Chung, R.M. (1985). "Influence of SPT Procedures in Soil Liquefaction Resistance Evaluations", *J. Geotech. Engrg. Div., ASCE*, **111**(12),1425-1445.

2. Stark, T.D. and Olson, S.M. (1995). "Liquefaction Resistance Using CPT and Field Case Histories", *J. Geotech. Engrg. Div., ASCE*, **121**(12), 856-869.

3. Robertson, P.K. and Wride, C.E. (1998). "Evaluating Cyclic Liquefaction Potential Using the Cone Penetration Test", *Can. Geotech. J.*, **35**(3), 442-459.

4. Shen, C.K., Vrymoed, J.L., and Uyeno, C.K. (1977). "The Effects of Fines on Liquefaction of Sands", *Proc. of 9th Int. Conf. on Soil Mech. and Found. Engrg. Tokyo*, **2**, 381-385, Japan.

5. Troncoso, J.H. and Verdugo, R. (1985). "Silt Content and Dynamic Behavior of Tailing Sands", *Proc. of 12th Int. Conf. on Soil Mech. and Found. Engrg., San Francisco, Calif.*, **3**, 1311-1314.

6. Finn, W.D., Ledbetter, R.H., and Wu, G. (1994). "Liquefaction in Silty Soils: Design and Analysis", Ground Failures under Seismic Conditions, Geotech. Spec. Publ., *ASCE*., **44**, 51-76.

7. Vaid, V.P. (1994). "Liquefaction of Silty Soils", Ground Failures under Seismic Conditions, Geotech. Spec. Publ., *ASCE*., **44**, 1-16.

8. Lade, P.V. and Yamamuro, J.A. (1997). "Effects of Nonplastic Fines on Static Liquefaction of Sands", *Can. Geotech. J.*, **34**(6), 918-928.

9. Yamamuro, J.A. and Lade, P.V. (1997). "Static Liquefaction of Very Loose Sands", *Can. Geotech. J.*, **34**(6), 905-917.

10. Zelatovic, S. and Ishihara, K. (1997). "Normalized Behavior of Very Loose Nonplastic Soil: Effects of Fabric", *Soils and Foundations*, **37**(4), 47-56.

11. Law, K.T. and Ling, Y.H. (1992). "Liquefaction of Granular Soils with Noncohesive and Cohesive Fines", *Proc. of 10th World Conf. on Earthquake Engrg.*, Madrid, **3**, 1491-1496.

12. Koester, J.P. (1994). "The Influence of Fine Type and Content on Cyclic Resistance", *Ground Failures under Seismic Conditions*, Geotech. Spec. Publ., *ASCE*, **44**, 17-33.

13. Ziaie-Moayed, R. (2001). "Evaluation of Cone Penetration Test Results in Loose Silty Sand", Ph.D. Thesis, Iran University of Science and Technology, Tehran, Iran.

14. Oda, M., Koishikawa, I., and Higuchi, T. (1978). "Experimental Study of Anisotropic Shear Strength of Sand by Plane Strain Test", *Soils and Foundations*, **18**(1), 25-38.

15. Ishihara, K. (1993). "Liquefaction and Flow Failure during Earthquakes", *Geotechnique*, **43**(3), 351-415.

16. Esna-ashari, M. (2005). "Evaluation of Liquefaction Potential of Silty Sands using Freezing Sampling Method and CPT Results", Ph.D. Thesis, Iran University of Science and Technology, Tehran, Iran.

17. Vaid, Y.P. and Sivathayalan, S. (2000). "Fundamental Factors Affecting Liquefaction Susceptibility of Sands", *Canadian Geotechnical Journal*, **37**(3): 592-606

18. ASTM D5311. (2002). "Standard Test Method for Load Controlled Cyclic Triaxial Strength of Soil", American Society of Testing and Materials, West Conshohocken, Pennsylvania, USA.

19. Norouzi, O. (2005). "Evaluation of Liquefaction Potential of Silty Sands in Cyclic Triaxial Tests", M.Sc. Thesis, Geotechnical Research Center, International Institute of Earthquake Engineering and Seismology (IIEES), Tehran, Iran.

20. ASTM D5311. (2002). "Standard Test Method for Performing Electronic Friction Cone and Piezocone Penetration Testing of Soils", American Society of Testing and Materials, West Conshohocken, Pennsylvania, USA.

21. Kayen, R.E., Mitchell, J.K., Seed, R.B., Lodge, A., Nishio, S., and Cotinho, R. (1992). "Evaluation of SPT,-CPT-, and Shear Wave-Based Methods for Liquefaction Potential Assessment Using Loma Prieta Data", *Proc. 4th U.S. Japan Workshop on Earthquake Resistant Design of*

Lifeline Facilities and Countermeasures for Soil Liquefaction, Honolulu, Hawaii, NCEER, Buffalo, NY, Technical Report NCEER, 92-0019, **1**, 177-204.

22. Seed, H.B. and Peacock, W.H. (1971). "The Procedure for Measuring Soil Liquefaction Characteristics", *J. Soil Mech. and Found. Div., ASCE*, **97**(SM8), 1099-1119.

23. Seed, H.B., Mori, K., and Chan, C.K. (1975). "Influence of Seismic History on the Liquefaction Characteristics of Sands", Report EERC 75-25, Earthquake Engineering Research Center, University of California, Berkeley.

24. Seed, H.B. and Idriss I.M. (1982). "Ground Motions and Soil Liquefaction during Earthquakes", Earthquake Engineering Research Institute Monograph, Oakland, CA.

25. Silver, M.L. and Seed, H.B. (1971a). "Deformation Characteristics of Sands under Cyclic Loading", *J. Soil Mech. and Found. Div., ASCE*, **97**(SM8),1081-1098.

26. Silver, M.L. and Seed H.B. (1971b). "Volume Changes in Sands during Cyclic Loading", *J. Soil Mech. and Found. Div., ASCE*, **97**(SM9), 1171-1182.

27. Lee, K.L. and Albaisa, A. (1974). "Earthquake Settlements in Saturated Sands", *J. Geotech. Engrg. Div., ASCE*, **100**(4), 387-406.

28. Pyke, R., Seed, H.B., and Chan, C.K. (1975). "Settlement of Sands under Multidirectional Shaking", *J. Geotech. Engrg. Div., ASCE*, **101**(4), 379-397.

29. Tokimatsu, K. and Seed, H.B. (1987). "Evaluation of Settlements in Sands due to Earthquake Shaking", *J. Geotech. Engrg. Div., ASCE*, **113**(8), 861-878.

30. Ishihara, K. and Yoshimine, M. (1992). "Evaluation of Settlements in Sand Deposits Following Liquefaction during Earthquake", *Soils and Foundations*, **32**(1),173-188.

31. Thevanayagam, S. and Martin, G.R. (2003). "Liquefaction and Post-Liquefaction Dissipation/ Densification Characteristics of Silty Soils", MCEER Highway Project, Task E2-1, Annual Report: Research Year 1.